SECTION E

MEASUREMENT OF SUSPENDED SOLIDS IN LAKES AND OCEANS USING SATELLITE REMOTE SENSING DATA

Dr. Michael Sydor
Department of Physics
University of Minnesota, Duluth
Duluth, Minnesota

o

INDEX

Abstract. E1
Method and Results. E2
Procedure for Remote Sensing Data Analysis. E7
Comparison of Calculated and Measured Radiance at Satellite Altitude E10
Figure Captions E12
Figures E15

o

MEASUREMENT OF SUSPENDED SOLIDS IN LAKES AND OCEANS USING SATELLITE REMOTE SENSING DATA

Investigator: Dr. Michael Sydor
Department of Physics
University of Minnesota, Duluth
Duluth, Minnesota

ABSTRACT

Using satellite remote sensing data to measure low concentrations of suspended solids in lakes and oceans requires careful evaluation of background signals from the atmosphere and the water surface. We present here typical background corrections for Lake Superior and determine the spectral distribution of the residual radiance from three major categories of turbidity in the lake. The results indicate that for large bodies of water, some general information on atmospheric scattering, water clarity, and the optical properties of suspended solids allows estimates of concentrations of suspended solids to within ± 0.5 mg/ℓ without using real time ground truth data. Under calibrated conditions the threshold detection level is 0.3 mg/ℓ for the fine particulates dispersed throughout the lake and 1 mg/ℓ for the highly light absorbing effluent from rivers. Comparisons of the minimum reflectance over the open lake areas with reflection from the highly absorbing tannin water from rivers, provides a check on the clarity of the atmosphere and the excessive background scatter from the water surface.

METHOD AND RESULTS

The spectral and the angular distributions of radiance from Lake Superior were measured with an optical probe which has a flat response from 400 to 900 nm. The detector had an acceptance cone of 5.65×10^{-2} steradians and an area of 1 cm^2. The spectral distributions of radiance were measured using a set of filters spanning the 380 to 1050 nm range. The filters had nominal band pass values of 10 nm. Measurements of the direct solar intensity were made with the probe and with an auxiliary narrow-angle NASA radiometer designed to measure the optical thickness of atmosphere.

The direct solar radiation per unit area normal to the incident solar ray is shown in Figure 1. The time of the measurements coincided with the LANDSAT 2 overpass. The sun elevation was 57°. The measurements represent average radiation for June 24, 26, 27, and 29, 1979. Curve 1 in Figure 1 is based on solar radiation values at the top of the atmosphere. The values are based on measurements by Thekaekara (1971) and are accepted as standard by NASA (Coulson 1975). Curve 2 shows the radiation at lake level.

The angular dependence of the radiation from Lake Superior was measured at several angles in the incidence plane (the plane containing the solar incidence ray and the normal to the water surface). The measurements were made looking towards the sun (forward angles), away from the sun (backscattered), and at right angles to the plane of incidence (side-scattered). Forward scatter is susceptible to glare and is not generally used in remote sensing of suspended solids. For light emerging at angles

near the Zenith, the backscattered and sidescattered radiances were similar when the sea conditions were calm. The radiances at the Zenith were devoid of the excessive specular reflection. However, at angles approaching 45° from the Zenith, the specular reflection of sky light overwhelmed the backscattered signal due to volume reflectance, as shown in Figure 2. The intensity and the spectral distribution of the overhead sky light, measured at 90° to the solar incidence along a line in the plane of incidence, are shown in Figure 3. The overhead sky intensity provides a measure of the specular reflection by the water surface. The specular reflection must be subtracted from radiance measurements to determine the residual radiance from the particulates. Figure 4 shows the spectral distribution of radiance for calm water containing less than 0.2 mg/ℓ of suspended solids. The radiances are measured near the nadir unless otherwise specified. The radiance in Figure 4 is broken down into the specular component, taken as 6% of the overhead sky intensity, and the remainder of the signal which is attributed to the volume scattering from the 0.2 mg/ℓ concentration of suspended solids. This remaining signal is assumed to be the volume reflectance by the carrying medium.

In analysis of remote sensing data for turbid water where concentrations exceed 1 mg/ℓ, the scatter from the carrying medium was diminished exponentially according to the ratio of secchi transparencies. The correction term is small, so the use of secchi transparencies is justified. Although the secchi transparencies are not precisely measureable, the parameter is a convenient and commonly available measure of the transparency of lakes and oceans. The decrease in the scatter from the carrying medium is important because it implies that for highly turbid or highly absorbing water, the background is due mainly to atmospheric scattering

and specular reflection by the water surface. This provides an important check on the clarity of the atmosphere and the clarity of water in the reference area when real time ground truth data are not available. For instance, when the minimum signal in the image is high because the reference area, assumed to be clear water, actually has turbidity on the order of 1 mg/ℓ, the corresponding residual radiance from the known areas of highly absorbing tannin water will be unusually low or negative in band 4 of the Landsat data. In a known system this will serve as a test of the assumption that the minimum reflectance area contains clear water. On the other hand, if the subtraction of the minimum radiance in the image yields residual radiances which are high in band 4 over the normally clear open lake areas and the areas with highly absorbing water, then the excessive background for the day is due to a turbid atmosphere.

The dependence of volume reflectance on angle is shown in Figure 5. The scatter is quite flat over the angles encompassing the range of LANDSAT observation angles and the acceptance angles for the probe, when measurements were made at or near nadir.

To obtain residual radiance due to turbidity, the measurements were corrected for surface and volume scattering according to Figure 4. As previously stated, the volume reflectance from the carrying medium was reduced exponentially according to the average secchi transparencies. Figures 6, 7 and 8 show the spectral distribution of the residual radiance for red clay, taconite tailings, and tannin. These are the dominant

111

types of suspended solids in Lake Superior. The fine red clay particulates shown in Figure 6 originate from extensive erosion along the Wisconsin shore of Lake Superior. Banks of clay are also present near Ontonagon, Michigan. Erosion of clay is the dominant natural source of inorganic particulates in the lake. The reflected sunlight peaks at 630 nm for the red clay. Red clay concentrations from 1 -15 mg/ℓ cover large sections of the lake, especially in extreme western Lake Superior.

Taconite tailings give a residual reflectance peak at 560 nm. The tailings are discharged from a point source at Silver Bay, Minnesota. The discharge, in excess of 6×10^4 tons/day, causes extensive plumes ranging in concentration from 1 to 4 mg/ℓ. Some of the fine tailings and the red clay particulates spread throughout the lake and form the main background of suspended solids in western Lake Superior.

Tannin is a term applied to the brown colored river water common around Lake Superior. Tannin is highly organic ($\sim$ 35%). It has low transparency, with secchi lengths ranging from .5 - 2 m in comparison with 3 - 5 m for western Lake Superior containing $\sim$ 1 mg/ℓ of red clay or tailings. The background clear water exceeds 10 m secchi transparency.

Figure 9 shows the spectral distribution of radiance from rough seas. It was obtained from the difference between radiance measured by looking into the wind (corresponding in this case to the sidescatter angles) and the backscattered radiance at right angles to the wind.

The spectral distribution of the residual radiances allow us to identify particulates in the lake (Sydor, Stortz, and Swain 1978). Using

the data in Figures 5 and 6 we can estimate the reflectance for each particulate type and concentration. We can also treat mixtures of particulates, since the reflectances are reasonably linear with the concentrations as shown for red clay in Figure 6. However, to be able to use the data in conjunction with the remote sensing information from the satellites, one needs to be able to predict the radiances at the satellite altitude. Furthermore, one needs to account for the seasonal changes in solar radiation at lake level and the attenuation of the residual radiance by the atmosphere. The attenuation by atmosphere can be obtained from Figure 1 by taking the ratio of the solar radiation at the lake and at the top of the atmosphere. The seasonal variation of the minimum background radiance from clear water and the atmosphere is shown by curve 1 in Figure 10. This variation arises mainly from the effects of solar elevation and changes of atmospheric attenuation at various solar angles (Coulson 1975). The broken line in Figure 10 approximates the effect of solar elevation and is given by

$$R = R_o(\cos\beta + \alpha\sec\beta)e^{-\mu\sec\beta}$$

where R is the radiance for clear water and clear atmosphere, β is the Zenith angle of the sun, α is the scattering coefficient for one atmosphere, and μ is the absorption coefficient for one atmosphere, which can be evaluated from Figure 1. The limits of fluctuation for background radiance are shown by curve 2 in Figure 10. The shape of curve 2 departs from the seasonal behavior during the winter. This departure can be attributed to rescattering. During the summer and fall the albedo over the lake is low. Thus correction for atmospheric rescattering of the light reflected from waters adjacent to the observation area can be

ignored. In the winter a high albedo from snow and ice packs surrounding the observed water area accounts for a substantial increase in the sky light intensity. In the summer and fall curve 2 also corresponds to the reflectance for .5 mg/ℓ of suspended solids and minimum atmospheric and surface background. In a sense curve 2, for May - November constitutes the average background radiance for the western Lake Superior. The .5 mg/ℓ concentration is an equilibrium concentration of particulates in extreme western Lake Superior. The open lake waters in western Lake Superior stay within the .2 - .8 mg/ℓ limits 97% of the time. Curve 2 is the upper limit on the acceptable background signal level for routine analysis of remote sensing data in the absence of the real time ground truth data. The atmospheric effects are most pronounced in band 4. For bands 5 and 6 only the best fit to minimum background values is given in Figure 10. Figure 11 shows the direct and diffuse components of solar radiation. The curves were obtained by fitting equation (1) to the minimum values of background radiation for clear atmosphere in bands 4, 5, and 6. This determined α, μ, and R_o. By scaling R_o to the value of solar radiation at the top of the atmosphere, we obtain solar radiation at lake level. The first term gives the direct component, while the second one approximates the diffuse component. The diffuse component is not the same as the total sky light.

PROCEDURE FOR REMOTE SENSING DATA ANALYSIS

When real time sampling data are available, the background signal can be calculated and subtracted from the image to produce residual radiances for the suspended solids. However in analysing satellite data

without ground truth, we first examine the image to locate the open lake area with the minimum signal. If the lowest intensity on the image for the open lake areas lies within the 0.2 mg/ℓ - .5 mg/ℓ limits shown in Figure 10, an assumption of .2 mg/ℓ suspended solids and clear atmospheric conditions is made. The residual radiance at satellite altitude is then obtained by subtracting from the image intensities the minimum background intensity given by curve 1 in Figure 10. The resulting data can subsequently be used to identify suspended solids to determine their concentrations according to Figures 6, 7, and 8. However, if the minimum signal in the image is substantially above the .2 - .5 mg/ℓ limits shown in Figure 10, a determination must be made of whether the background is high because of high overall turbidity of the water or because of excessive atmospheric scattering. Visual examination for extensive plumes, thin clouds or haze can be made. Normally, only tapes with clear images of the lake are purchased. However, a test of excessive background signal levels can be made by first subtracting from the image the minimum background according to curve 1, Figure 10, and then examining whether the excess in the background has the spectral character attributable to the atmosphere (according to Figure 11), rough seas (Figure 9), or suspended solids, (according to Figures 6, 7, and 8). If the spectral dependence of the excess in background indicates that the atmosphere is turbid, the satellite data may still be usable provided the atmospheric turbidity is uniform. However, the resulting error for the estimates of concentration of suspended solids can be as high as 1 mg/ℓ and the identification of the suspended solids at low concentrations will be hampered because of the unpredictable spectral behavior of the turbid atmosphere.

The unambiguous identification of the suspended solids relies on identifying the spectral shape of the residual radiance, and it requires a signal at least two or three digital steps above background. This in turn requires that the horizontal concentration gradients in suspended solids be large enough to provide a change of 1 mg/ℓ for red clay and tailings and of 3 mg/ℓ for tannin, over the entire area of the lake covered by the image. Such gradients are readily available for most images containing near shore areas and are usually satisfied in the images of Great Lakes. However, this condition does impose some bothersome restrictions. In Lake Superior, for example, tannin concentrations in the lake must be usually compared with those in the Duluth harbor, or a comparable tannin area large enough to be well resolved in the image.

Although unambiguous identification of particulates from LANDSAT data cannot be made for concentrations lower than 1 mg/ℓ in absence of ground truth data, estimates of suspended solids concentration can be made to within .5 mg/ℓ above background. Furthermore, some decisions on the identity of particulates can also be made at those concentration levels. When no ground truth is available, but the lowest reflectance over the lake is within the clearly acceptable background limits, the assumption of .2 mg/ℓ concentration for the lowest intensity area introduces a probable error of ± .3 mg/ℓ in the estimates of concentration of red clay and the tailings. The identity of the low concentration of suspended solids can also be deduced from spectral dependence based on magnitude of signals in two bands. For western Lake Superior, for instance, the background is usually red clay or tailings, so the decision on the identity of the low concentration of particulates in the lake can be made by examining the relative magnitude of the signal in bands 4 and

5. For the tannin water, which usually has higher intensity in band 6 than band 4, the identity can be based on the relative signal in bands 6 and 4. Unfortunately, concentrations of tannin lower than 1 mg/ℓ cannot be detected in LANDSAT data. At high concentrations, various algorithms can be devised to automatically extract from the residual radiances the identity and concentrations of the suspended solids. Figures 12, 13, and 14 show application of previously published algorithms (Sydor, Stortz, and Swain 1978) to the data for June 29, 1979. The identity of suspended solids in the image agrees closely with the sampling data all along the transects of our 1979 cruise of the western Lake Superior.

COMPARISON OF CALCULATED AND MEASURED RADIANCE AT SATELLITE ALTITUDE

To examine how well the results in the previous sections can be used to analyse remote sensing data, we calculate the radiances at the satellite altitude and compare them with the satellite data for specific sampling sites on Lake Superior. The sampling points are shown in Figure 15. These points correspond to some of the stations for our 1979 experimental cruise of Lake Superior using research vessel Crockett.

The predicted radiance values shown in Table 1 are close to the observed satellite values. The corrections for atmospheric attenuation were taken into consideration according to Figure 1. The satellite data were obtained from the Canada Centre for Remote Sensing. The Canadian data for LANDSAT 2 provides a signal resolution level of 1/255.

Some results discussed in previous sections are evident from Figure 15 and Table 1. Notice, for instance, that the signal level in band 4 for the Duluth harbor tannin water is lower than the signal in the open

Station		Minimum Background at Satellite			Residual Radiance at Ground			Residual Radiance at Satellite			Expected Radiance at Satellite			Landsat 2 Radiances		
Western Lake Superior	Landsat Bands	4	5	6	4	5	6	4	5	6	4	5	6	4	5	6
	Clean Water	.26	.11	.07				.06	.04	.01				.32	.15	.08
A	Tailings 1.8 mg/ℓ	.26	.11	.07	.124	.089	.026	.11	.08	.021	.37	.19	.09	.37	.18	.09
B	Red Clay 8 mg/ℓ	.26	.11	.07	.196	.21	.07	.175	.19	.06	.44	.30	.13	.45	.29	.13
C	Tannin 3 mg/ℓ	.26	.11	.07	.093	.096	.045	.083	.086	.036	.34	.20	.11	.35	.21	.11

Radiances in mw/(cm^2SR)

Overall background turbidity in western Lake Superior shows spectral character most like tailings having concentration 1 mg/ℓ - actual value .8 mg/ℓ. Tailings at station A 1 mg/ℓ above background - just on the verge of positive identification from Landsat data.

Table 1.

E11

118

lake areas. This indicates excessive background. Thus in absence of real time ground truth data, a check on the lowest background signal could have been made to ascertain the clarity of the atmosphere or the clarity of the open lake water. In this case it would have shown that the overall turbidity of the lake was high. The spectral character of the residual signal for low intensity open lake areas indicates, according to Table 1, approximately a 1 mg/ℓ background of tailings. Actually the open lake was more turbid than normal, having a background suspended solids of level of .7 mg/ℓ of tailings. Thus it is realistic to assume that for background conditions falling within the accepted values shown in Figure 10, an estimate of the suspended solids could be made to within ± .5 mg/ℓ in absence of the ground truth data. Nimbus G data promise to provide an even better sensitivity for Lake Superior work. However, the angular dependence for the volume and surface scattering may be more difficult to handle in the Nimbus G data. In anticipation of Nimbus G data, it is interesting to compare the spectral shape for the difference in volume reflectances observed at a 40° Zenith angle, for 8 mg/ℓ and 14 mg/ℓ red clay concentrations. This difference is shown in Figure 16. We notice that measurements at Zenith for the 5.6 mg/ℓ concentration yield a similar spectral response. We might thus expect that for Zenith angles smaller than 40° (Figure 2), we might still be able to use remote sensing data from the Nimbus Coastal Zone Scanner to identify the particulates in plumes, without resorting to elaborate models for angular scattering by small particulates.

FIGURE CAPTIONS

Figure 1. Direct solar radiation at lake level. The experimental values represent 4 day averages. Measurements were made in .01 μm bands spaced at 05 - .08 μm intervals. Curve 1 shows the reference radiation at the top of the atmosphere, which is based on standard N.A.S.A. values derived from measurements by Thekaekara (1971).

Figure 2. Angular distribution of 0.4 - 0.9 μm light backscattered and specularly reflected from clear lake water (.2 - .5 mg/ℓ suspended solids). Measurements were made in the plane of incidence with the instrument pointing away from the sun. Specular reflection of sky light becomes dominant at Zenith angles exceeding 40°.

Figure 3. Diffuse overhead solar radiation measured in the plane of incidence, along a line perpendicular to the incident sun ray. The sun was at 23° Zenith angle.

Figure 4. Curve 1 shows the spectral distribution at nadir of the radiance from clearest lake water (less than .2 mg/ℓ suspended solids). Curve 2 shows the fraction of this radiance attributable to specular reflection of the overhead sky light by the calm water surface.

Figure 5. Laboratory determination of the angular distribution of .646 μm light scattered by fine red clay particulates and fine mining waste particulates. These particulates are the prevalent constituent of suspended solids in western Lake Superior.

Figure 6. Spectral distribution at nadir of light reflected from red clay turbidity in Lake Superior. The residual radiance from particulates is linear for concentrations of suspended solids lower than 10 mg/ℓ.

Figure 7. Spectral distribution at nadir of light reflected from mining tailings. Tailings often upwell from a broad deposit of discharge slurry at the bottom of the lake.

Figure 8. Spectral distribution at nadir of light reflected from highly organic, opaque river water commonly referred to as tannin. The above turbidity contained .5 mg/ℓ of red clay particulates.

Figure 9. Spectral distribution at nadir of light scattered from rough seas (white caps). The reflectivity has a flat spectral dependence. Rough seas can be easily identified in remote sensing data because of their high reflectance at long wavelengths (.8 - 1.1 μm) and unstructured geometric patterns.

Figure 10. Seasonal behavior of the background radiance due to light scattered by the atmosphere, the water surface, and the low concentration of particulates in clear water (.2 mg/ℓ suspended solids). The volume scatter by the clear water is taken as the intrinsic scatter by the carrying medium. Curve 1 represents LANDSAT derived measurements of radiance in band 4 (.5 - .6 μm) for the clearest atmospheric conditions. Curve 2 corresponds to the maximum value of acceptable radiance from clear water and uniform atmosphere - defining the clear viewing conditions when straightforward analysis for suspended solids may be made in absence of real time ground truth data. The broken line in band 4 corresponds to the seasonal dependence of radiance as a function of sun elevation. The curves for band 5 (.6 - .7 μm) and band 6 (.7 - .8 μm) show average radiance for clear viewing conditions. The minimum cutoff radiance in bands 5 and 6 for LANDSAT 2 and 3 is indicated by the dotted lines.

Figure 11. Curves 1, 2, and 3 show the calculated values of direct solar radiation at lake level for bands 4, 5, and 6 respectively. Curves A, B, and C give the respective total solar radiations in bands 4, 5, and 6, including the diffuse component from the overhead sky. The experimental points represent measurements of the direct solar radiation plus the fraction of forward scattered sunlight included within the acceptance angle of the instrument.

Figure 12. Distribution of red clay particulate (in excess of .5 mg/ℓ) in western Lake Superior. The identifications for suspended solids are based on the relative magnitudes of the residual LANDSAT intensity readings in bands 4, 5, and 6 and the ratios of the residual intensities.

Figure 13. Distribution of mining waste tailings in the 1 - 1.5 mg/ℓ range.

Figure 14. Distribution of output from the St. Louis River (lower left corner) into western Lake Superior. The output from smaller rivers in Wisconsin can also be seen along lower shoreline.

Figure 15. Band 4, LANDSAT 2 digital output averaged over 90 pixels. Note the low readings in the lower left corner of the image showing the St. Louis River estuary and the Duluth harbor. The overall turbidity in the lake is higher than average, thus opaque river water shows lower apparent background than the open lake areas.

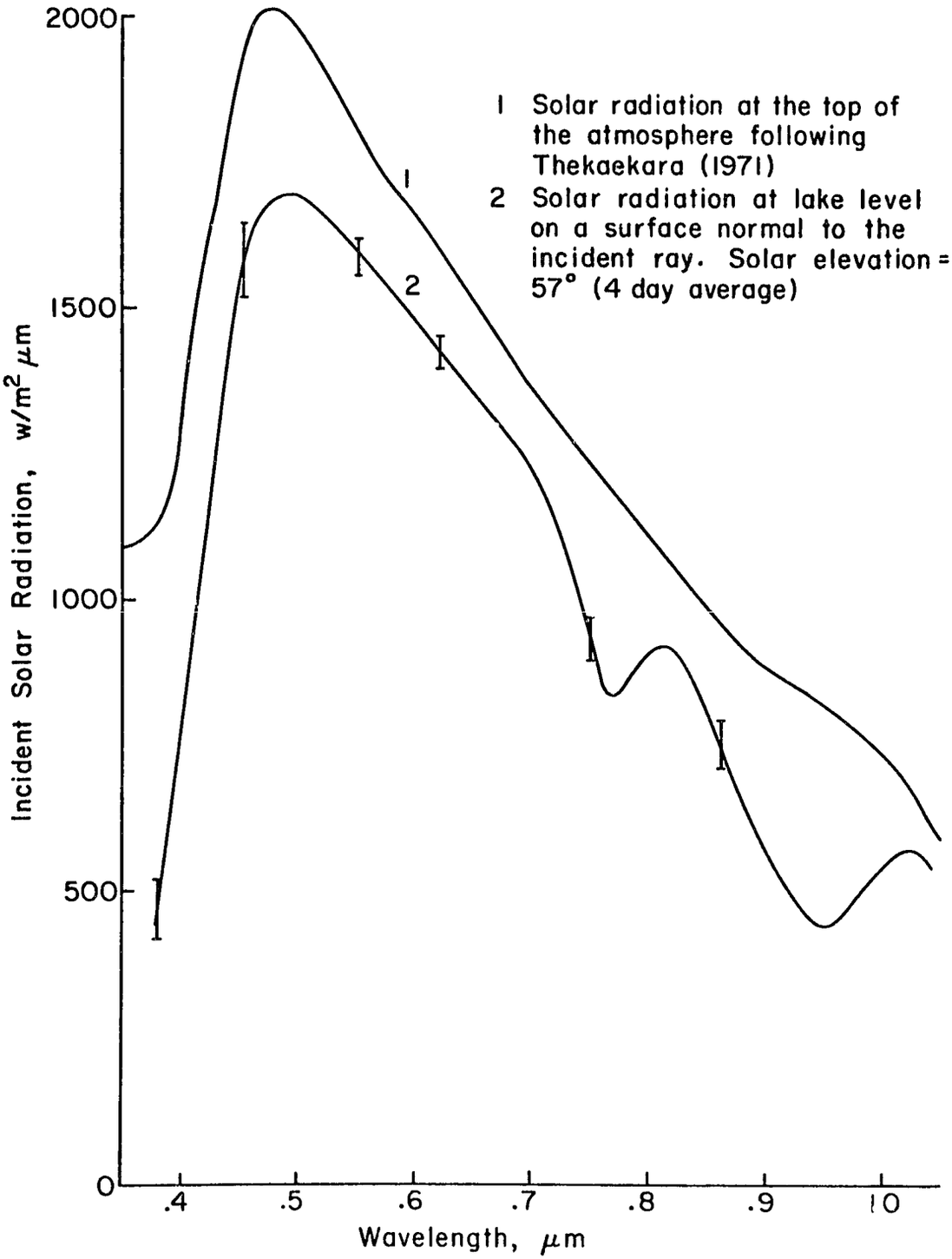
2000
1500
1000
500
0
Incident Solar Radiation, w/m² μm
.4
.5
.6
.7
.8
.9
1.0
Wavelength, μm
1
2
1 Solar radiation at the top of the atmosphere following Thekaekara (1971)
2 Solar radiation at lake level on a surface normal to the incident ray. Solar elevation = 57° (4 day average)

Figure 1

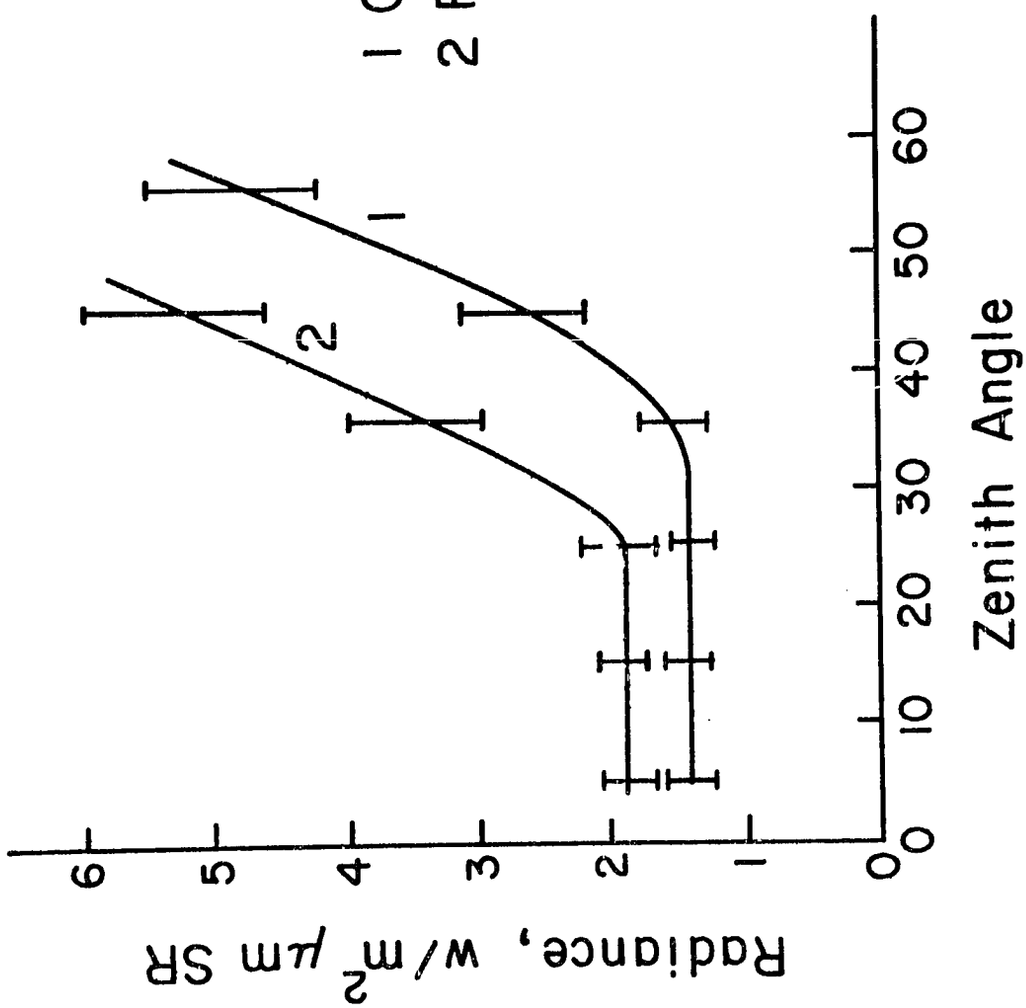
1 Calm seas
2 Rough seas
1
2
Radiance, w/m² μm SR
0
1
2
3
4
5
6
0
10
20
30
40
50
60
Zenith Angle

Figure 2

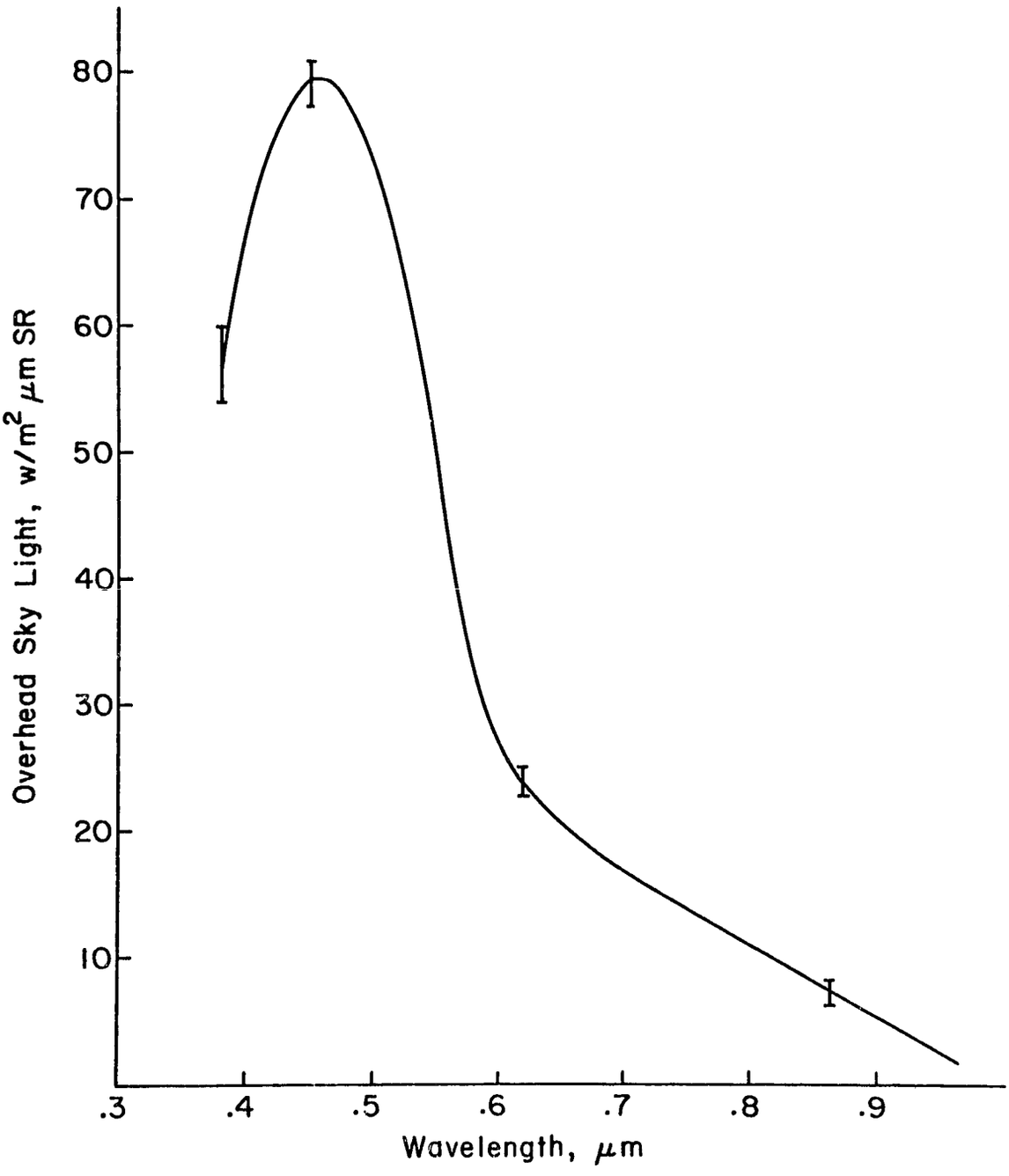
Overhead Sky Light, w/m² μm SR
80
70
60
50
40
30
20
10
.3
.4
.5
.6
.7
.8
.9
Wavelength, μm

Figure 3

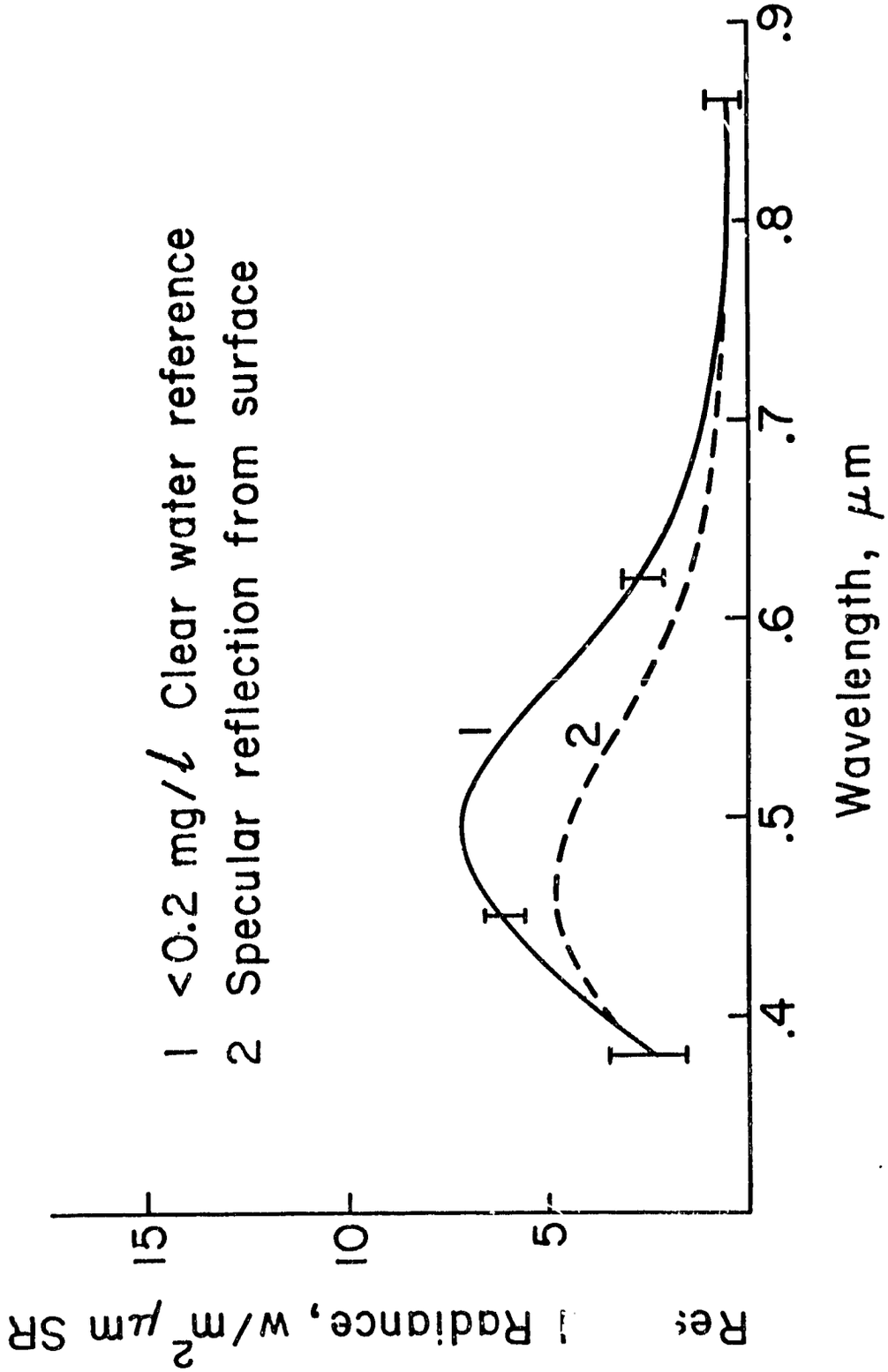
1 <0.2 mg/l Clear water reference
2 Specular reflection from surface
Wavelength, μm
.4
.5
.6
.7
.8
.9
5
10
15
Radiance, w/m² μm SR

Figure 4

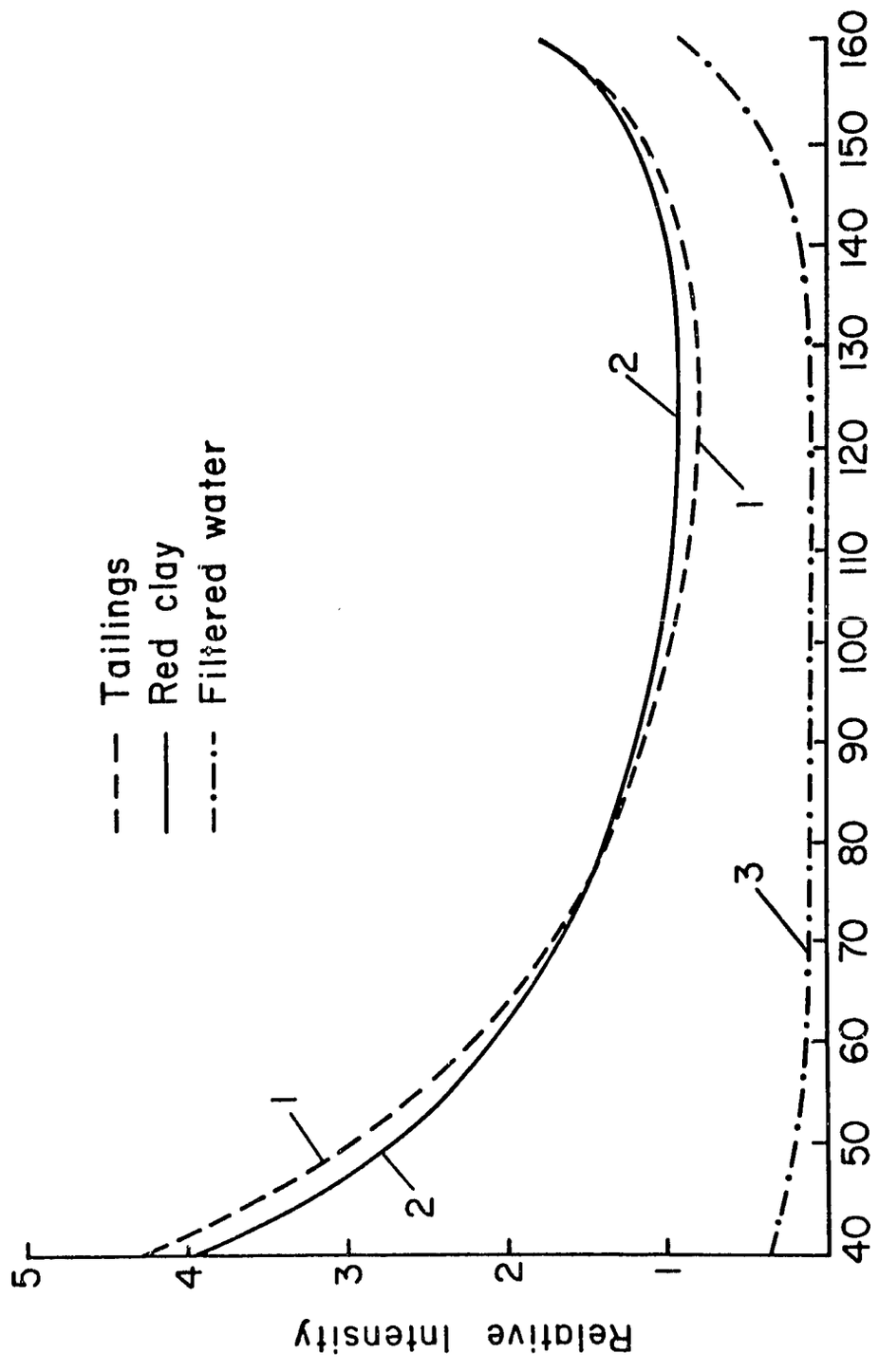
Tailings
Red clay
Filtered water
Relative Intensity
Scattering Angle
5
4
3
2
1
40
50
60
70
80
90
100
110
120
130
140
150
160
1
2
3
1
2

Figure 5

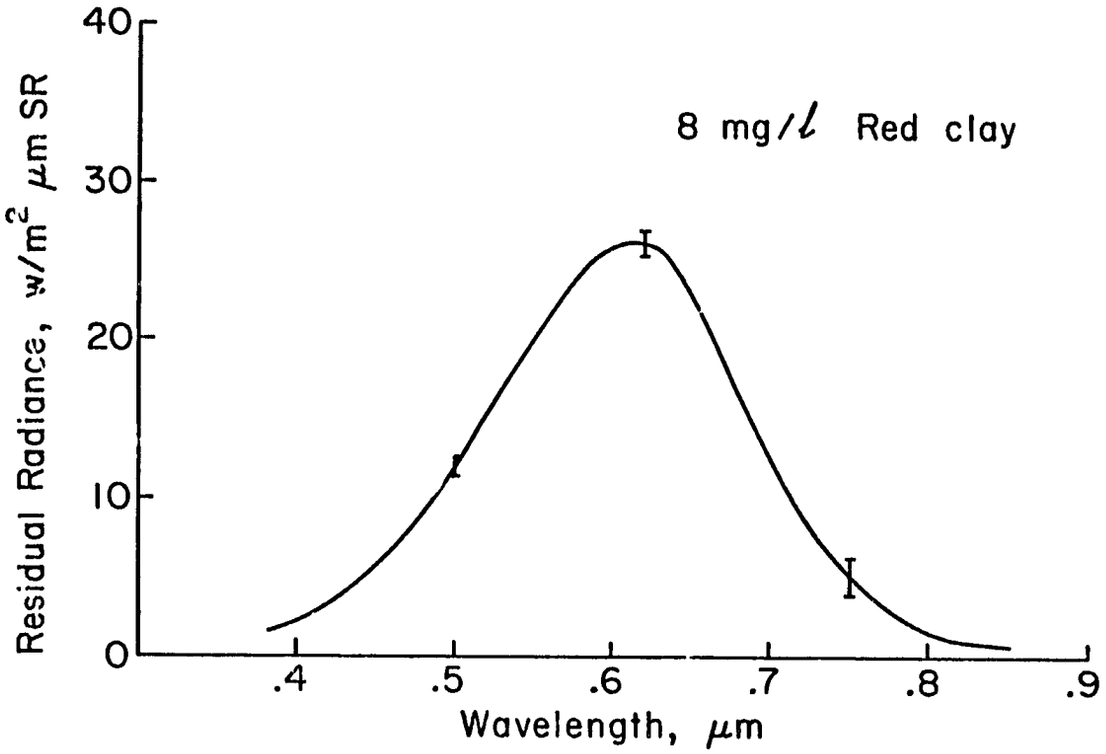
8 mg/l Red clay
Residual Radiance, w/m² μm SR
40
30
20
10
0
.4
.5
.6
.7
.8
.9
Wavelength, μm

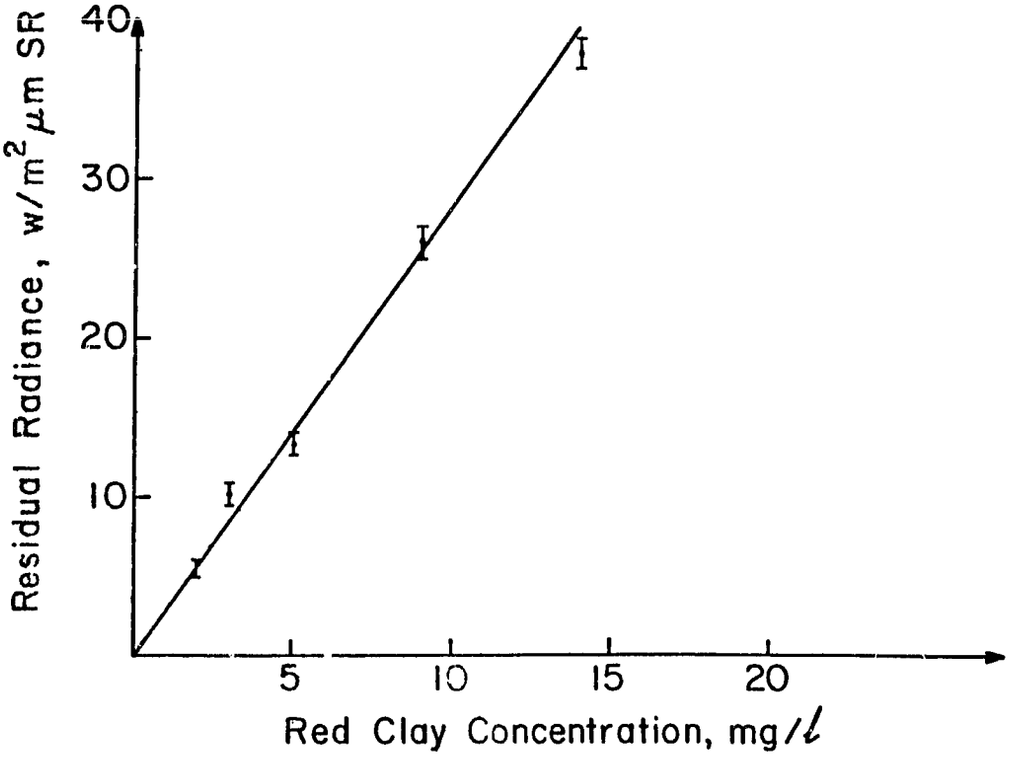
Residual Radiance, w/m² μm SR
40
30
20
10
5
10
15
20
Red Clay Concentration, mg/l

Figure 6

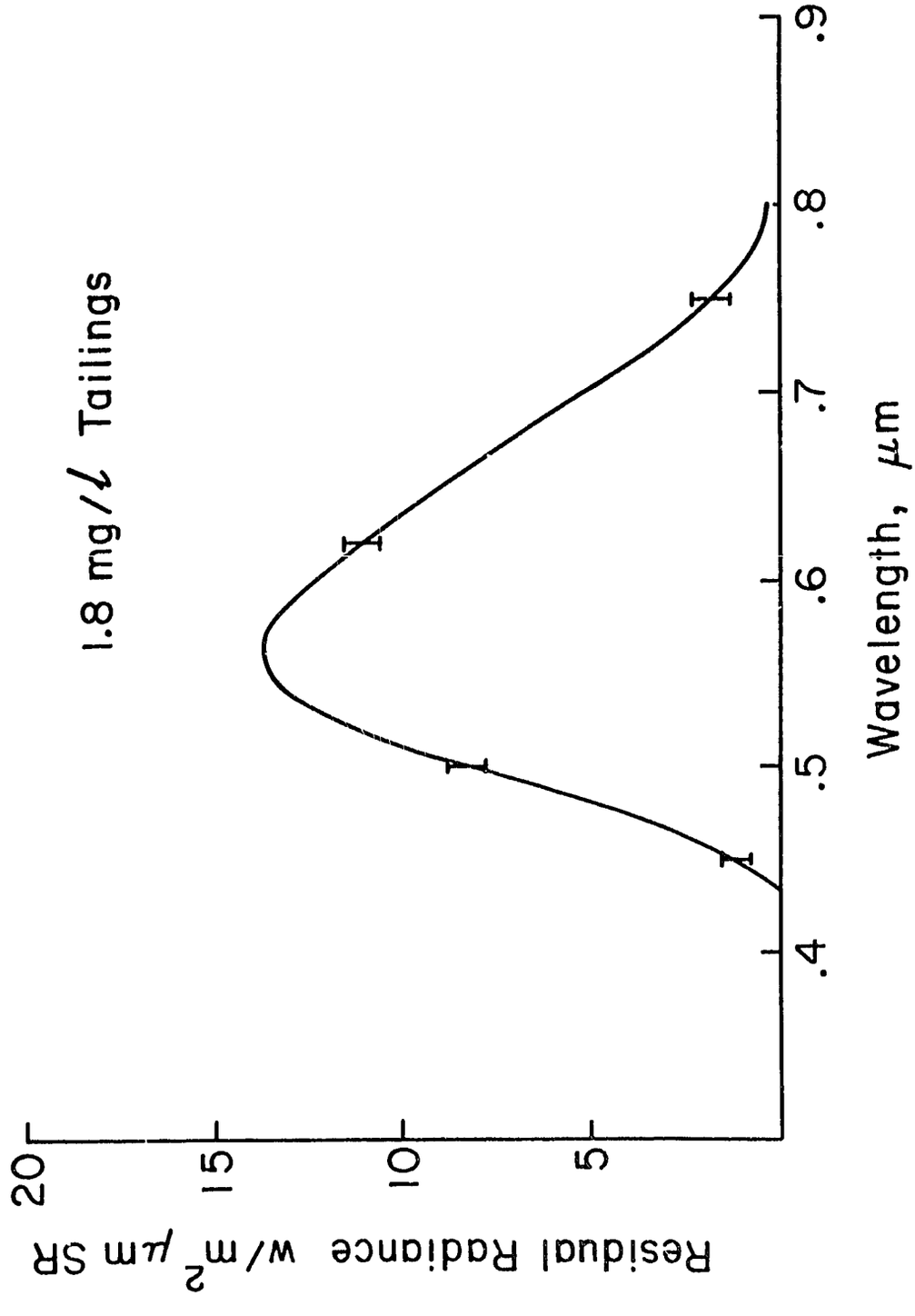
1.8 mg/l Tailings
Residual Radiance w/m² μm SR
20
15
10
5
.4
.5
.6
.7
.8
.9
Wavelength, μm

Figure 7

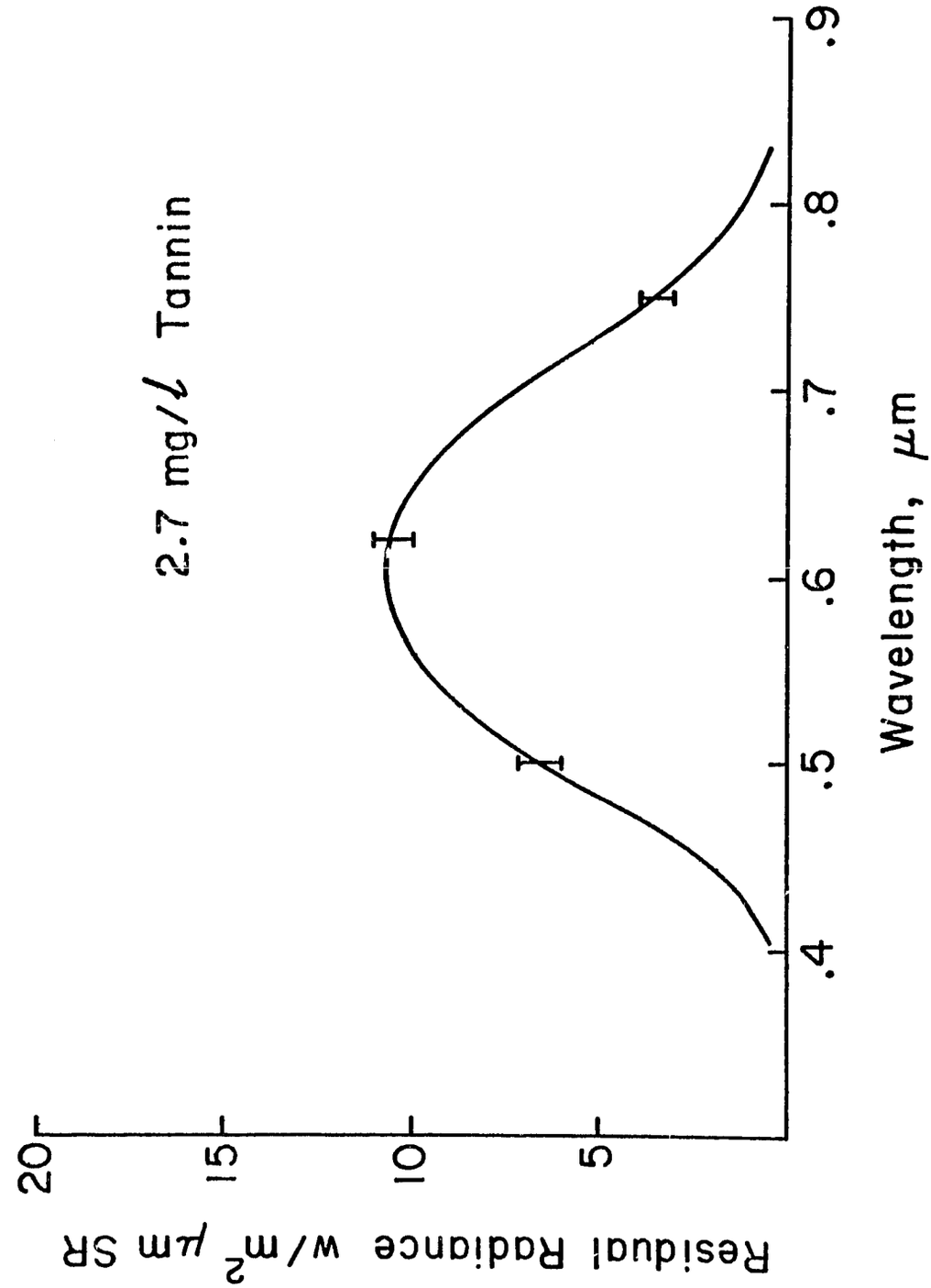
2.7 mg/l Tannin
Residual Radiance w/m² μm SR
20
15
10
5
.4
.5
.6
.7
.8
.9
Wavelength, μm

Figure 8

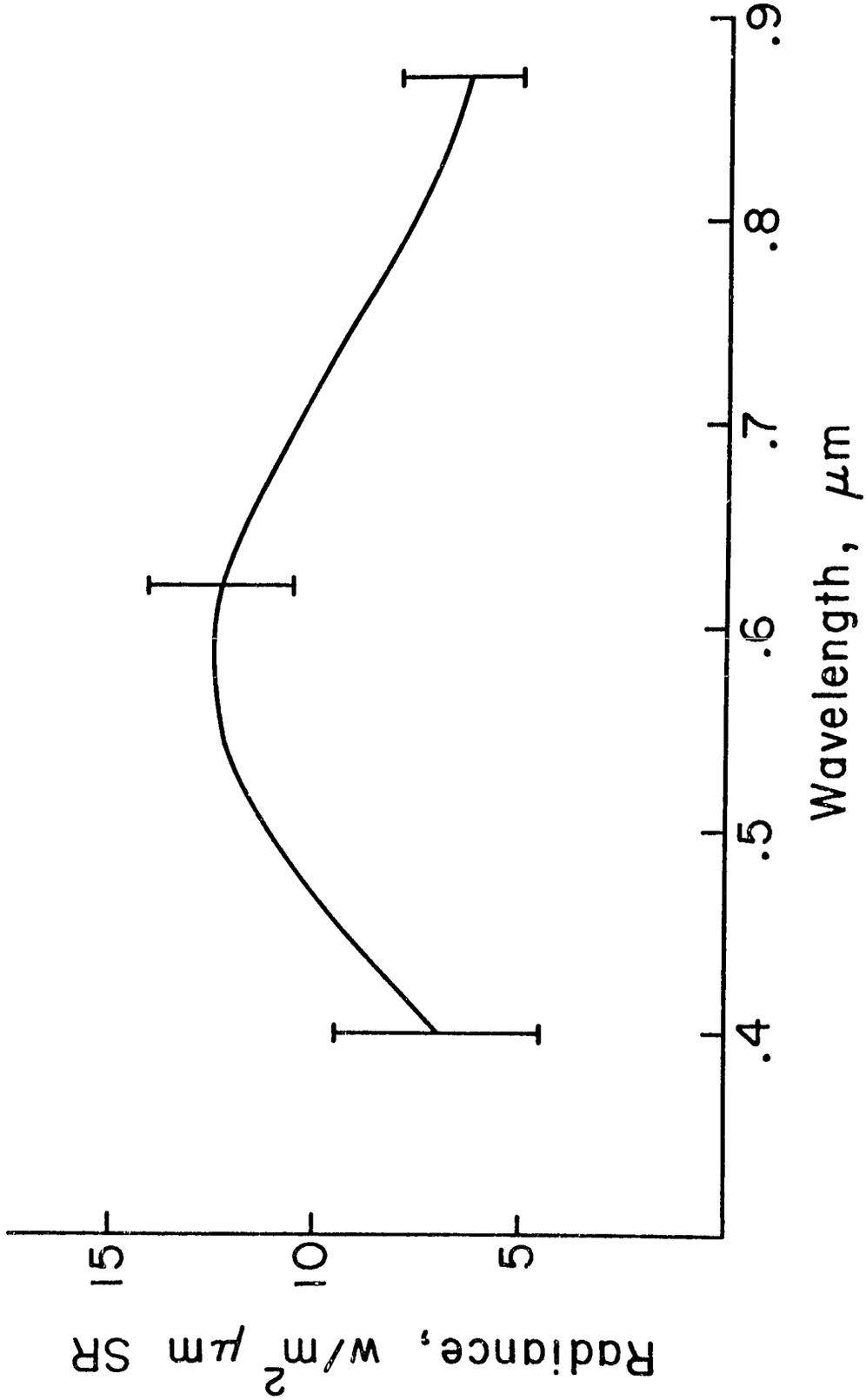

Figure 9

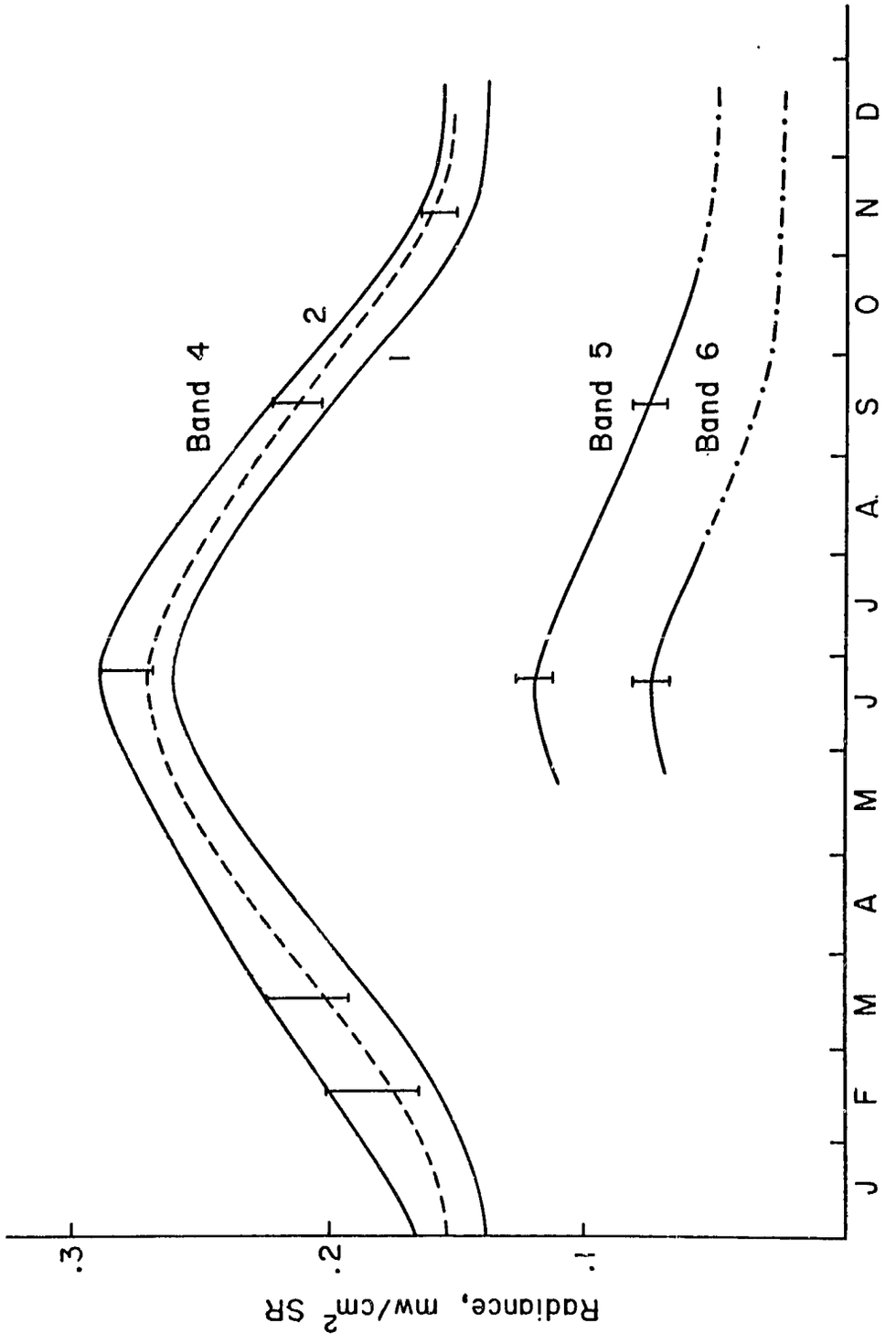
Band 4
2
1
Band 5
Band 6
J F M A M J J A S O N D
Month
.3
.2
.1
Radiance, mw/cm² SR

Figure 10

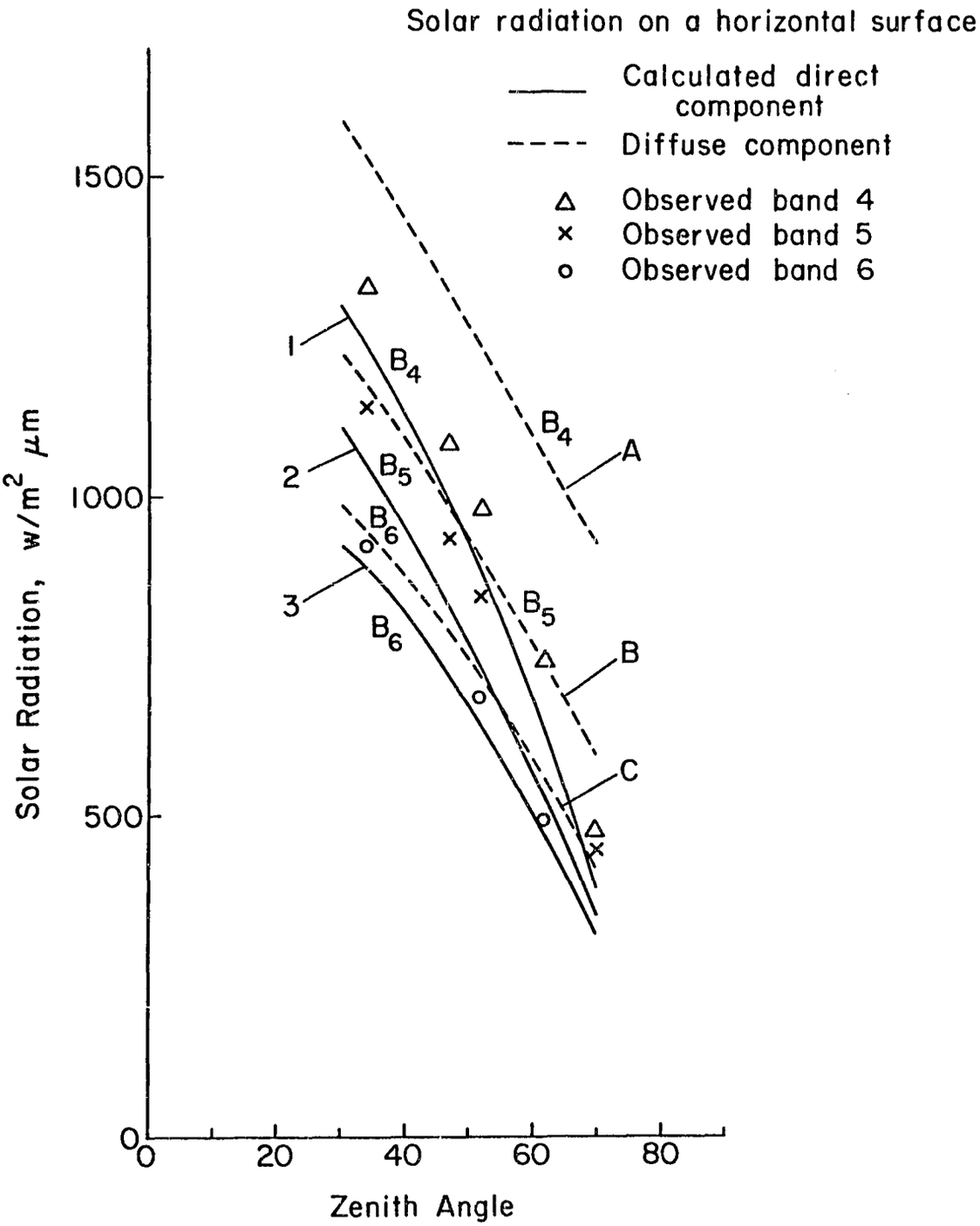
Solar radiation on a horizontal surface
Calculated direct component
Diffuse component
Observed band 4
Observed band 5
Observed band 6
Solar Radiation, w/m² μm
1500
1000
500
0
0
20
40
60
80
Zenith Angle
1
2
3
B4
B5
B6
A
B
C

Figure 11

Figure 12

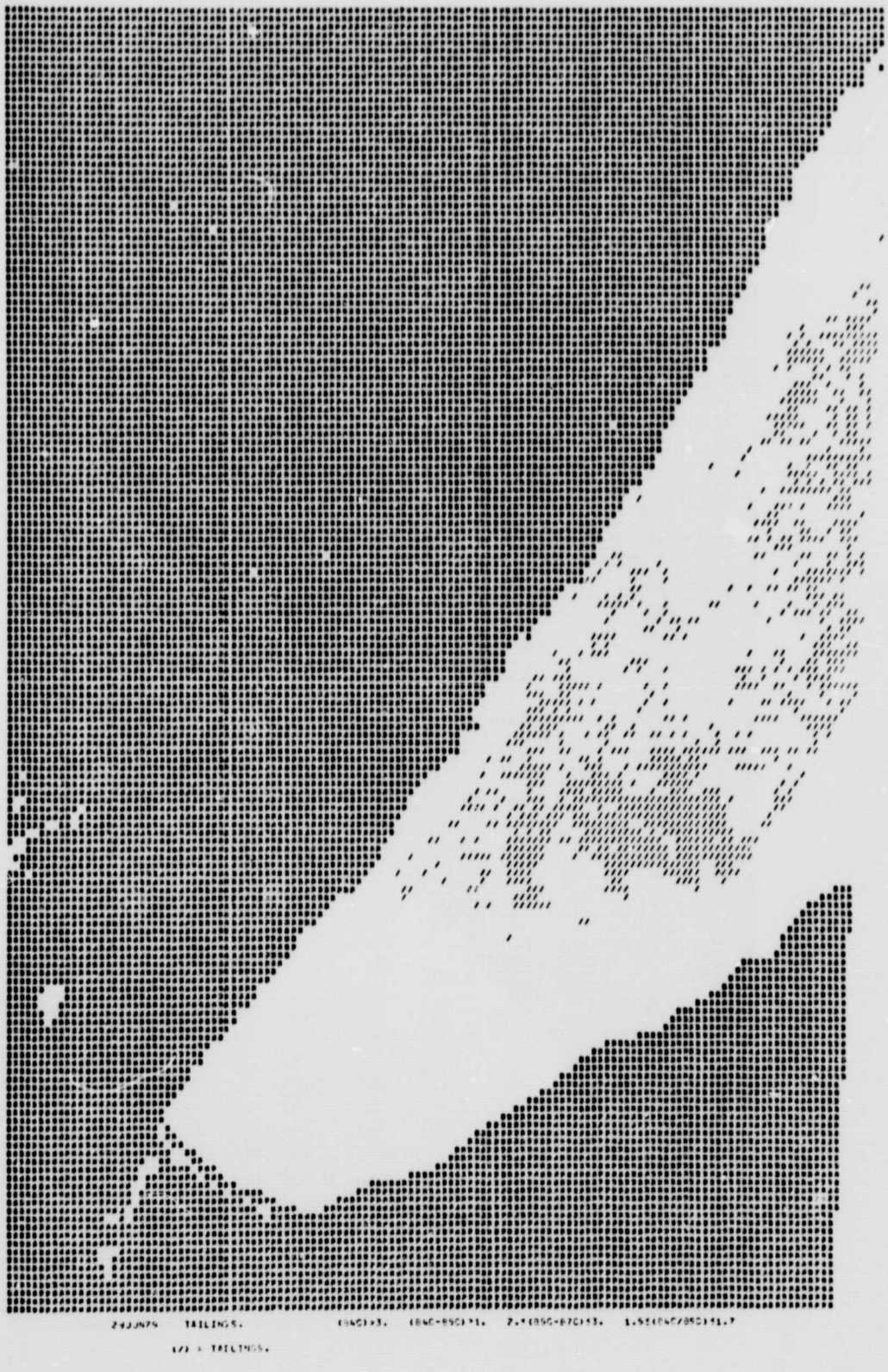

Figure 13

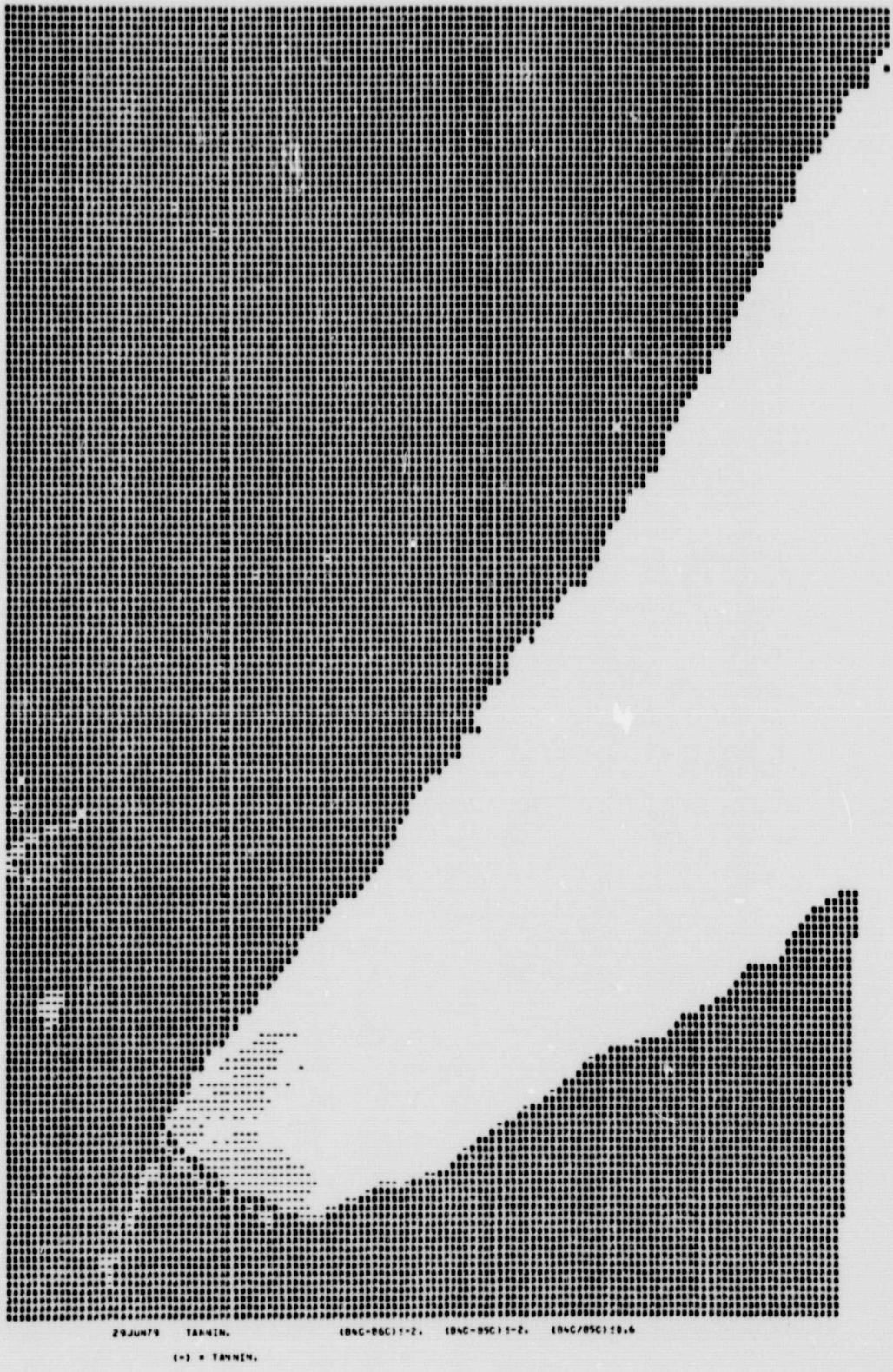

Figure 14

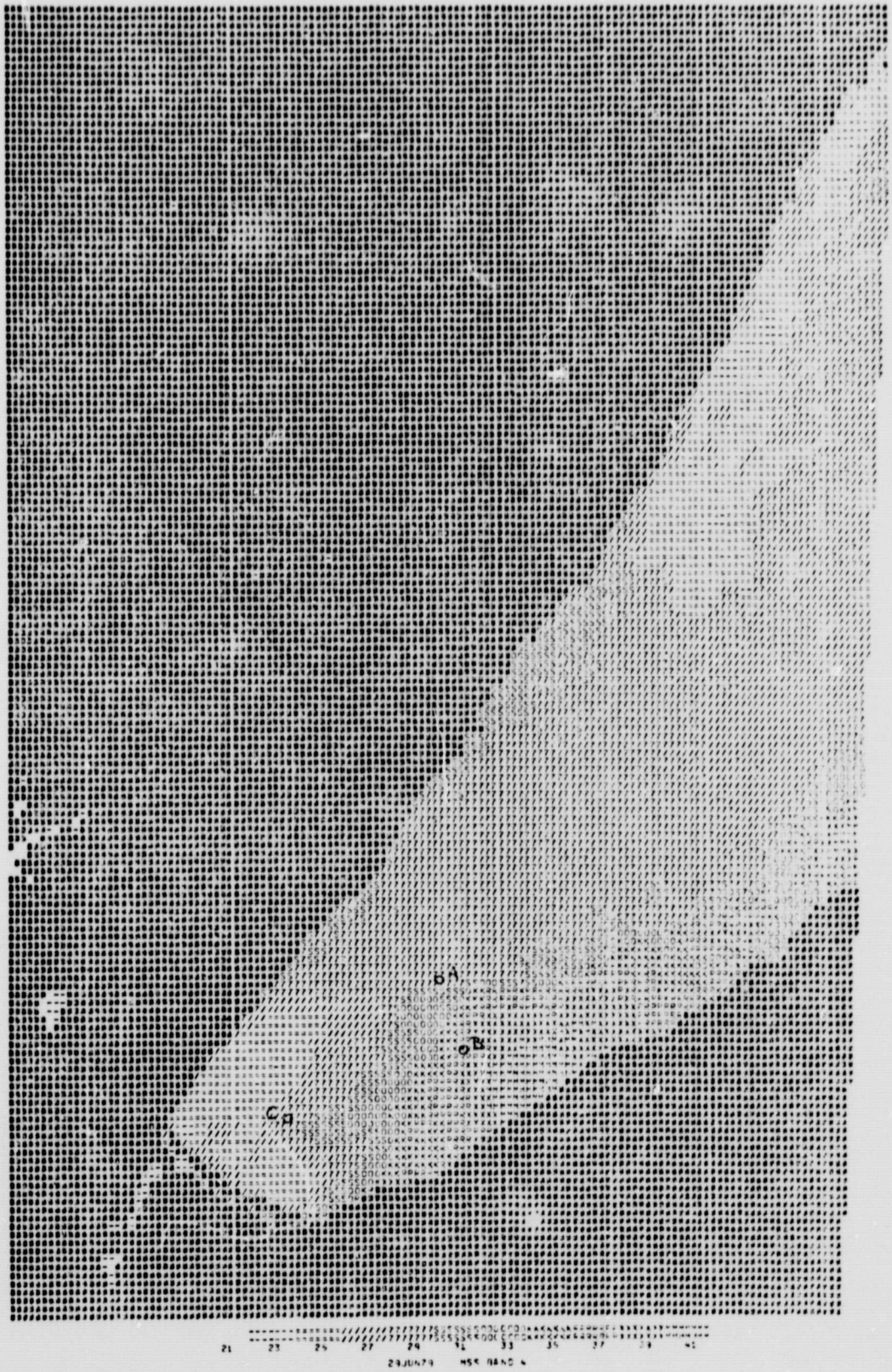

Figure 15